Transverse electron focusing as a method for investigating the Andreev reflection

V. S. Tsoĭ, N. P. Tsoĭ, and S. E. Yakovlev

Institute of Solid-State Physics, Academy of Sciences of the USSR, Chernogolovka, Moscow Province

A transverse focusing method was developed for investigating the Andreev reflection (AR). The main advantages of the method are an opportunity for the study of the reflection of a local group of electrons on the Fermi surface and the ability to generate electron and hole excitations and to vary their energy in a wide range. The method provides means for direct observation of a change in the type of excitation in the AR case and for direct determination of the AR probability, and of its energy and angular dependences. It is therefore possible to investigate normal–superconducting (*n–s*) interfaces and the characteristics of the interaction of excitations with an *n–s* interface. A study was made of the AR at a bismuth–tin interface. Direct observations were made of a change in the type of excitation in the AR process. The AR probability was determined for the bismuth–tin interface and was found to be close to 1 for excitation energies less than the energy gap, indicating that the investigated interface was of sufficiently high quality. The energy dependence of the AR probability was determined.

Transverse electron focusing[1] is an effective method for the investigation of the scattering of conduction electrons on the surface of a sample.[2] This method can be used to study the scattering of conduction electrons on internal surfaces, particularly the Andreev reflection (AR) from a normal–superconducting (*n–s*) metal interface.[3-5] Effective methodological methods have been developed for the study of the AR. In addition to the traditional methods (involving measurements of the thermal and electrical resistance), the AR is now being investigated employing the rf size effect,[6-9] current-voltage characteristics of microjunctions,[10-13] attenuation of ultrasound,[14] and electron focusing.[3-5] The rf size effect can be used to observe directly the AR (Ref. 6). The electron focusing method provides means for direct observation of a change in the type of excitation in the AR case[3] and for the study of the dependence of the AR probability on the excitation energy.[5] The microjunction technique involving the use of a point made of a normal metal in contact with a superconductor[10] or a point made of a normal metal in contact with a thin plate or film of a normal metal coated on the opposite side with a superconductor,[11-13] can be used to study the dependence of the AR on the excitation energy. Methods which are differential in respect of the position of electrons on the Fermi surface can provide more detailed information on the AR. Discovery of the high-temperature superconductivity has drawn attention to the AR at an *n–s* interface between two different substances.

The electron-focusing effect was used by us to develop a differential method for the investigation of the AR, which was then applied to the AR from an *n–s* interface between bismuth and tin.

METHOD

Samples. The most stringent requirement in respect of the selection of suitable material for a sample is the condition $l(\varepsilon) \sim L$, which is necessary for the investigation of the energy dependence of the AR (l is the mean free path of electrons, L is the distance between the contacts, and ε is the excitation energy). It is desirable to satisfy this relationship by selecting a material with the maximum value of $l(\varepsilon)$, since a reduction in L increases the magnetic field $H \propto I/L$, which limits further the range of usefulness of the method, because it excludes superconductors characterized by low critical magnetic fields. It is reasonable to use therefore a metal with a high permittivity $\varkappa$ since $l(\varepsilon) \propto \varkappa^{-1}$. One of them is bismuth characterized by $\varkappa \sim 100$. Another important advantage of bismuth is a low density of conduction electrons (10^{-5} electrons per atom) so that the magnetic fields needed to observe the electron focusing effect are at least an order of magnitude weaker than those required in the case of ordinary metals.

In our experiments we used two types of bismuth single crystals in which the C_3 axis was perpendicular to the surface of a sample: disks 2 mm thick grown in a polished quartz demountable mold[15]; a single crystal grown by the Czochralski method with two plane-parallel surfaces about 1 cm wide, one of which was the working surface. The cross section of a crystal was an elongated figure with the ratio of the extremal dimensions 1:5. The superconductor material was tin. Tin dissolves with difficulty in bismuth and has a very low coefficient of diffusion in bismuth, particularly along the C_3 axis. The superconducting transition temperature of tin is $T_c = 3.73$ K, which is convenient when experiments are carried out both above and below T_c.

An *n–s* interface, involving deposition of a tin film by evaporation, was formed in ultrahigh vacuum. Use was made of a UNI-5 system made by Rieber and provided with a chamber where samples were prepared, an ion gun, Auger and mass spectrometers, and a slow-electron (low-energy) diffractometer. The base pressure in the chambers was $\sim 10^{-9}$ Torr and the main residual gases were N_2, CO, and H_2. The surface of a sample was cleaned by bombardment with argon ions. The argon pressure in the chamber was $\sim 10^{-4}$ Torr. During surface cleaning the chamber was pumped out by a titanium sublimation pump, which was chemically passive in respect of rare gases. We used two types of cleaning techniques: the ions energies were 150 and 300 eV. Polishing (etching) time was ~ 1.5 h at 150 eV and 1 h at 300 eV. After etching, the samples were annealed for 4 h at temperatures of 180 and 200 °C, respectively. Cleaning of the surface with 300 eV ions left a chemically pure surface on which the concentration of impurities was below the sensi-

tivity of the Auger spectrometer. However, this procedure was insufficient to determine on which surface one could observe visually the process of low-energy electron diffraction (LEED). After cleaning the surface by bombardment with 150 eV ions, it was found that only a few oxygen and carbon impurities remained and annealing of the surface made it possible to observe visually the LEED patterns. The intensity in the diffraction pattern, the relationship between the amplitudes of the reflections in the background, and the energy profiles of the intensities were similar to those observed in a LEED study of the (111) face of antimony.[16]

The experiments were carried out on samples with thick (several thousands of angstroms) and thin (less than 1000 Å) tin films. In the case of the thick film, in spite of the fact that the average thickness was much less than the probe depth, the amplitude of the Auger peak of bismuth (at 103 eV) decreased by just 30% compared with the amplitude before the deposition of the film by evaporation. Hence, we concluded that the tin film was of island nature and that bismuth was possibly segregated. Moreover, we observed the LEED pattern of the bismuth substrate on which a (6×6) reconstruction took place. After the film deposition a sample was taken out of the ultrahigh-vacuum chamber and further manipulations were carried out under normal conditions. The thin film was removed around the contacts by subjecting the point electrode to a voltage of ~ 100 V. Sometimes this procedure had to be repeated several times. In the case of the thick film it was not possible to use this method in order to establish a contact which was not shunted to the superconducting film. Regions free of the tin film were then formed by a photolithographic technique. A system of alternate photoresist stripes was established on the surface of a sample. The width of the stripes and the separation between them were 0.15 mm. Then, an acid was used to etch away the tin film from the parts of the surface which were not covered by the photoresist. After a time an n–s interface became degraded as manifested by the fact that the presence of the film did not affect electron focusing. In the case of the thick film the initial properties were retained for several years, whereas in the case of the thin film the corresponding period was several months.

Measuring head. A measuring head was used to make contact with the surface of a sample in the AR investigations to satisfy more stringent requirements than in studies of the conventional reflection; this was due to the fact that the contacts should be established with specific parts of the surface of the sample and should be separated by a small distance. The difference of our measuring head from that described earlier[17] was the ability to displace the point electrodes and the sample along additional directions and to check visually the positions of the points and the state of the surface of a sample.

Figure 1 shows the main components of the measuring head. Sample 1 was attached to a mobile stage, which was displaced by a screw 2 along the x axis. An emitter E was attached to a beam 3 which was fixed firmly to a support. The beam 3 acted as an elastic spring so that the position of E was governed by the position of a screw 4, which could be rotated to displace E along the z axis. A collector C was attached to another beam 5. The beam 5 was fixed to a beam 6 and the beam 6 was attached to a support with the aid of needle positioners 7, which in practice prevented their mutu-
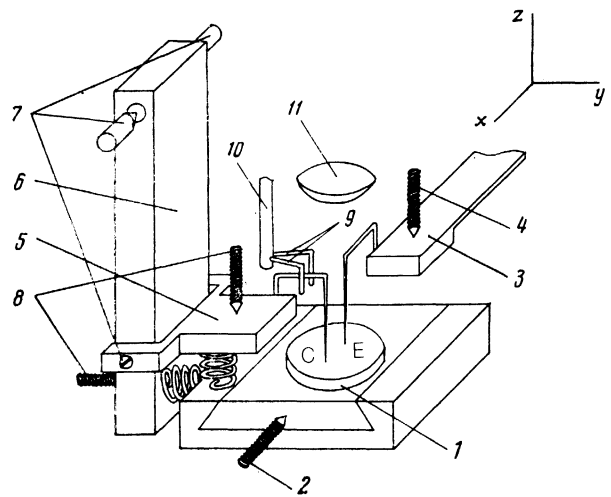
FIG. 1.

al arbitrary displacement. Screws 8 and a rod 10 with a fork 9 were used to move the collector C along the x, y, and z axes. The point electrodes in the sample could be displaced as necessary at helium temperatures. The screws were rotated via reducing gears, which made it possible to displace various components in steps of the order of one micron. Inside a cryostat we used transparent glass Dewars which made it possible to check the position of the points with the aid of a microscope located outside the cryostat. Moreover, an objective 11 and an eyepiece (not shown in Fig. 1) were located outside the cryostat and used to monitor the positions of the points and the state of the surface of the sample between the contacts after cooling of helium below the λ point (the ob-
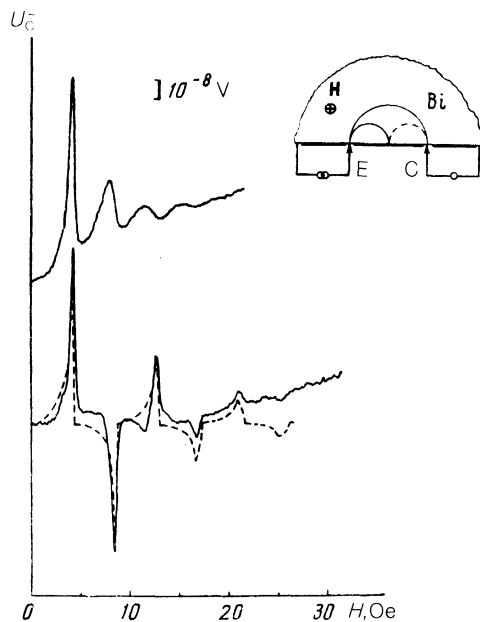
FIG. 2. Dependence of U_C on H at $T = 4.2$ K (upper curve) and at 1.7 K (curves displaced arbitrarily downward on the ordinate scale). The dashed curve gives the results of calculations of electron focusing in the multiple AR case. The calculations were made assuming that the dimensions of the emitter E and the collector C are the same and also that $b/L = 0.04$, $l/L = 0.5$, $q = 0$, and $Q_1 = 0.58$. A film of tin is represented by the thick line in the inset.

servations were made under a magnification of $\times 100$). The minimum distance between the contacts was $\sim 40\,\mu$m.

Measuring circuit. The experimental setup is shown schematically in Fig. 2. The emitter E and collector C contacts were located along the C_2 axis, whereas a magnetic field **H** was applied in the plane of the sample and perpendicular to C_2. An electric current $I_{\tilde{E}} = I_{\tilde{0}} \sin \omega t$ (of frequency $\omega \sim 10^3$ rad·s^{-1}) was passed through E and measurements were made of $U_{\tilde{C}}$, which was the amplitude of the alternating voltage on the collector C. In the adopted experimental geometry the first electron focusing line was formed by nonequilibrium electrons from one of the three Fermi surface ellipsoids of bismuth, which were emitted by E and reached C without reflection by the surface. The second electron focusing line and those of higher orders were formed by electrons reflected by a sample-surface part coated by a tin film. The dependence of the nature of the reflection process on the excitation energy was determined by a modulation method[18]: the dependence of the amplitude of an electron focusing line on the direct current $I_E^=$ was determined:

$$I_E = I_E^= + I_0{}^\sim \sin \omega t; \quad I_0{}^\sim = \text{const} \ll I_E^=.$$

The acceleration voltage was $U_E^= = R_E I_E^=$. In the experiments the emitter resistance R_E was about 1 Ω, and the current used in the monitoring measurements was $I_0^\sim = 2\cdot10^{-5}$ A.

CHANGES IN THE NATURE OF EXCITATIONS UNDER THE ANDREEV REFLECTION CONDITIONS

The type of carrier generated at the emitter E was governed by the polarity of the applied voltage. When the polarity was such that conduction electrons were accelerated in the region of E, then electron excitations (electrons) were generated, whereas the opposite polarity ensured creation of holes. At the excitation focusing point there was a peak of the potential and the polarity of this peak was determined by the type of excitation. In the AR case the velocity vector and the signs of the charge and mass of an excitation were reversed, i.e., in the AR case there was a change specifically in the type of excitation. When there was no change in the nature of focused excitations, the polarity of the voltage on C was the same as that on E. An obvious consequence of this is an alternation of polarities of the electron focusing lines in the AR case because of a change in the type of excitation, i.e., the polarity of the odd electron focusing lines involving participation of excitations reflected an even number of times from the surface was identical with the polarity of the first line; the even lines had a different polarity, because they were formed by a different type of carrier than that responsible for the first electron focusing line. The problem in question was analyzed theoretically in Ref. 19. The change in the polarity of the second electron focusing line due to the AR was observed experimentally earlier.[3] The technique described above made it possible to observe electron focusing in the case of the multiple AR. Figure 2 shows the dependence of $U_{\tilde{C}}$ on the magnetic field under the following conditions: $L = 0.2$ mm, $T = 1.7$ K, $I_E^\sim = 1$ mA, and $I_E^= = 0$. We were able to observe the first six electron focusing lines of the AR in which the polarities of the even and odd lines were opposite.

The electron focusing lines for the multiple AR were observed for samples with a thin tin film and only for relatively high values of L ($> 100\,\mu$m). At lower values of L the electron focusing lines were nominally not observed even after the double AR. This was clearly due to the fact that the size d_n of the region around the point free of a tin film amounted to $\sim 60\,\mu$m. The same estimate of d_n was obtained from an analysis of the data in Fig. 2 ($d_n/2 = L/6 = 30$ μm). The reflection of the excitations responsible for the electron focusing lines labeled 7, 8, ... occurred on the defective part of the surface near the point, which was free of the tin film, so that these lines could not be resolved. When a defective surface was formed deliberately in this way between E and C (Ref. 17), a similar effect was observed: the electron focusing lines numbered 3, 5, or higher were suppressed; it was governed by the position and width of the defective part of the surface.

In the multiple AR the nth electron focusing line was observed in a field nH_0, where H_0 is the field in which the first line was observed. This was due to the fact that reversal of the sign of the charge of the excitations was accompanied by a reversal of the sign of the mass.

ANDREEV REFLECTION PROBABILITY

Since only a small group of electrons participated in the formation of an electron focusing line, observation of such lines as a result of the multiple AR made it possible to determine experimentally the AR probability for a local group of electrons on the Fermi surface. We shall consider the formation of an electron focusing line in the multiple AR case employing the geometric model of electron focusing[17,20] and assuming a spherical Fermi surface. According to this geometric model, the voltage on the collector U_C is governed by the flux of the "effective" electrons accelerated in E and reaching C either without collisions with the surface of a sample or after specular reflection by the surface. In the AR case the voltage U_C is governed by excitations reaching the collector either without collisions with the surface or after the AR from the n–s interface.

We shall assume that E is a point electrode and the characteristic size of C is b. We can easily see that the first electron focusing line is due to excitations moving almost normally to the surface of a sample within a solid angle $\Omega \propto (b/L)^{3/2}$. In the momentum space the angular size of the region on the Fermi surface from which electrons reach C in a plane parallel to **H** and perpendicular to the surface is $\sim b/L$, whereas in a plane orthogonal to **H** and to the surface the corresponding size is $\sim (b/L)^{1/2}$; this is the reason for the power exponent 3/2 in the expression for the solid angle. In the case of specular reflection by the surface the amplitude of the nth electron focusing line is $A_n = A_1 q^{n-1}$, where q is the specular reflection probability, since the nth electron focusing line is formed by the same excitations as the first line. The probability that this occurs is allowed for by the factor q^{n-1}. The situation changes radically in the AR case because in each of the two consecutive jumps on the surface an excitation is displaced in a magnetic field in different directions. Therefore, the displacement along a magnetic field of those excitations which are responsible for the even electron focusing lines is small and the limitations on the solid angle Ω in a plane parallel to **H** are due to the fact that the displacement s of excitations at right angles to **H** (along L) is such that

$L - b < s < L + b$. In this case we have

$$A_{2n} \sim \left(\frac{b}{L}\right)^{1/2}\left(\frac{b}{L}\right)^{1/2} Q_A^{2n-1};$$

where Q_A is the AR probability.[3]

In the case of the odd electron focusing lines the displacement of one jump along **H** is not compensated. The situation is similar to the case of specular reflection, but the displacement time of an excitation along **H** represents $1/(2n+1)$th part of the time taken to travel from E to C. We therefore have

$$A_{2n+1} \sim \min\left\{(2n+1)\left(\frac{b}{L}\right)^{3/2}; \frac{b}{L}\right\}Q_A^{2n}.$$

For known values of A_n, there are obvious formulas relating Q_A to the ratio of the amplitudes of the electron focusing lines. In the case of the even lines, we have

$$Q_A = (A_{2m}/A_{2n})^{1/2(m-n)}; \quad m, n = 1, 2, \ldots; \quad m > n.$$

The expression for A_n depends on the shape of the Fermi surface. The simplest situation occurs in the case of a cylindrical Fermi surface, which in practice describes bismuth. The motion of excitations then occurs in a single plane perpendicular to the cylinder axis; the limitations from the solid angle Ω are imposed by the condition $L - b < s < L + b$ for lines of all the numbers both in the AR case and in the case of ordinary reflection, and we then have

$$Q_A = (A_m/A_n)^{1/(m-n)}.$$

Figure 3 shows the dependence of the logarithm of the amplitude of the electron focusing line for the AR on its number, which is described satisfactorily by the above expression (in the coordinates of Fig. 3 it should be a straight line). In this case the ratio of the amplitudes of the adjacent electron focusing lines is independent of their serial numbers and amounts to 0.50 ± 0.15.
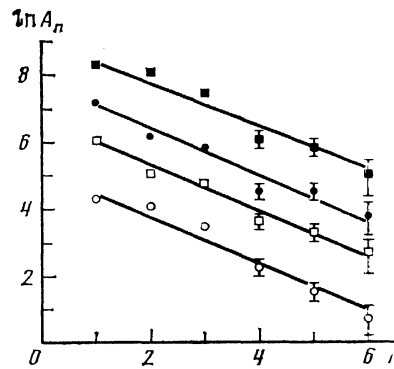
FIG. 3. Dependence of the logarithm of the amplitude of the electron focusing lines $\ln A_n$ on the line n. Different symbols are used for measurements on different parts of the surface. The error of these measurements is indicated in those cases where it exceeds the size of the symbol.

The above expressions for Q_A deduced from the ratio of the amplitudes of various electron focusing lines are valid in the case of a homogeneous n–s interface. For real surfaces in the case of ordinary reflection and a randomly homogeneous surface the value of q is governed in particular by the statistical characteristics of a rough surface. The situation is radically different for the AR. The special feature of the AR is that the surface roughness does not determine the amplitude of an electron focusing line in the AR case,[3] because, firstly, the direction of the local normal to the surface does not govern the direction of reflection of a quasiparticle; secondly, the minimum size of the irregularities of a rough surface, which is of the order of the correlation length, is governed by the roughness of the n–s interface. The amplitude of an electron focusing line for the AR case is governed by the statistical characteristics of the n–s interface, including the fraction of the area of the n–s interface in the investigated part of the surface of a sample. It should be mentioned that specularly reflected excitations make a negative contribution to the am-
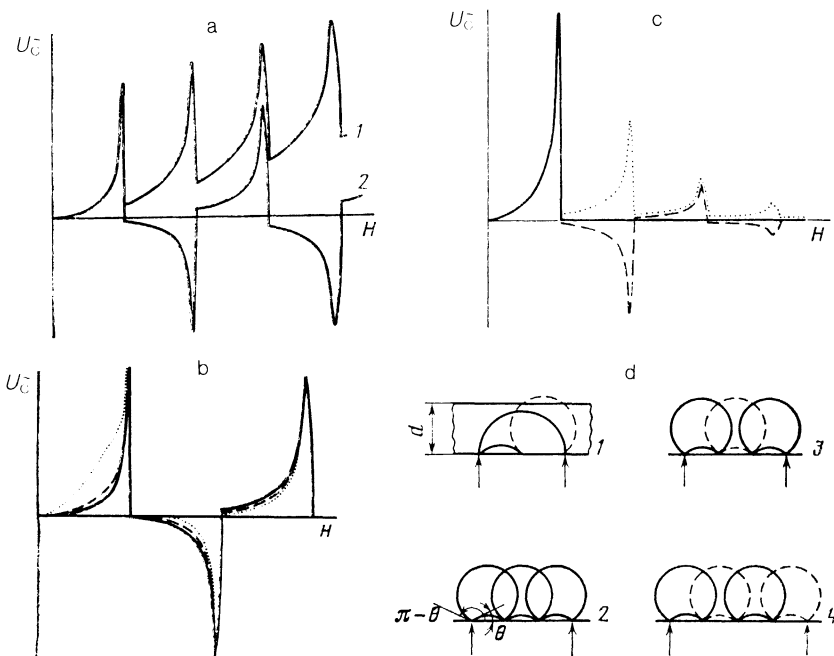
FIG. 4. Calculations of electron focusing made using the geometric model (a–c): a) $q = 1$, $Q_A = 0$ (1), $q = 0$, $Q_A = 1$ (2); b) $q = Q_A = 0.5$ (continuous curve), $q = 0.3$, $Q_A = 0.7$ (dashed curve), $q = 0.7$, $Q_A = 0.3$ (dotted curve). The first electron focusing line is practically the same for all three cases; c) l/L is equal to 1 (continuous curve), 0.5 (dashed curve), or 0.25 (dotted curve). The ordinate scale is selected for different curves in such a way that the functions coincide at the maxima. d) Paths of excitations of different types in a sample of thickness d are shown by continuous and dashed curves.

plitude of an electron focusing line for the AR. Figures 4a and 4b give the results of calculations of the amplitudes of electron focusing lines obtained using the geometric model of electron focusing on condition that the specular and Andreev reflections occur at the interface: $q + Q_A = 1$. The ratio of the amplitudes of electron focusing lines is $|q - Q_A|^{m-n}$. The polarity of the even electron focusing lines is governed by the sign of this difference. If $q = Q_A$, only the first electron focusing line is observed. We shall use q_A to denote the AR probability deduced from the ratio of electron focusing lines. There are also several other factors (discussed below) which make it possible to distinguish q_A from Q_A.

If $U_E^= = 0$, the deviation of q_A from unity may be due to, in particular, two factors: 1) in the presence of a potential barrier at the n–s interface which governs $Q_A(0)$ (see below) and, consequently, $q_A(0)$; 2) the island nature of the tin film, so that some fraction of the investigated reflecting surface represents the n–s interface, which reduces q_A and this reduction is not due to a reduction in Q_A. A reduction in the fraction of the surface of bismuth not covered by the tin film and exclusion of an insulating spacer between bismuth and tin should increase both q_A and Q_A. Clearly, it is the maximum value of q_A that actually represents the Bi–Sn interface. In the description of the method we mentioned that the tin film was of the island type. Magnification in an electron microscope was insufficient to resolve the structure of the film. The width of the LEED reflections indicated that the dimensions of the patches on the substrate free of the tin film were not less than the coherence length of the electron beam, which was ~ 100 Å. In the opposite case we should observe additional broadening of the reflections due to the size of the part of the surface forming the diffraction pattern. Observation of electron focusing when the point electrode was brought into contact with different parts of the surface indicated that the surface was strongly inhomogeneous. In some cases the value of q_A^- was close to 1. Clearly, it was this value that represented the "perfect" Bi–Sn interface and was equal to Q_A.

The results plotted in Fig. 3 thus demonstrated the following. The surface of a sample between the contacts was statistically homogeneous; it had a patchy structure and 50% of the surface was covered by a tin film forming an n–s interface between Bi and Sn. In an analysis of electron focusing in the multiple AR the Fermi surface of bismuth could be regarded as cylindrical.

DIRECTION OF THE VELOCITY OF EXCITATIONS IN THE ANDREEV REFLECTION

An obvious method for observing changes in the direction of the velocity vector of excitations in the AR (in contrast to the specular reflection case there was reversal of the sign of all the components of the velocity vector) is to carry out experiments on thin samples and record the singularities due to the cutoff of the electron orbits that do not fit within a thin plate; this is illustrated schematically in Fig. 4d. The singularity should be observed for an arbitrary nature of the process of electron reflection from the opposite surface of the plate; moreover, the AR gives rise to an additional electron focusing line.[4]

Indirect information on changes in the direction of the

velocity vector in the AR is provided by experiments on electron focusing as a result of the multiple AR. The essence of such experiments is the change in the path λ of an effective electron between E and C as a result of the AR. In the specular reflection case (shown schematically as 2 in Fig. 4d) the path traveled by an effective electron emerging from E at an angle θ (or $\pi - \theta$) is equal to $2R\theta n$ [or $2R(\pi - \theta)n$], where n is the number of jumps and R is the radius of the electron path. In the AR case when the number of jumps is odd we have $\lambda_{2n+1} = 2\pi Rn + 2R\theta$ [or $2\pi Rn + 2R(\pi - \theta)$], whereas for an even number of jumps we find that $\lambda_{2n} = 2\pi Rn$ (3 and 4 in Fig. 4d). In view of the finite value of l, the probabilities that the excitations travel from E to C are different for different values of λ and this gives rise to the following properties. The relative amplitude of the electron focusing lines should not change because in all cases a line is formed by excitations with $\lambda \approx \pi L/2$. However, the shape of the line and particularly its width can change significantly: in the specular reflection case the profiles of the different electron focusing lengths are similar and only the scale changes proportionally to the line numbers; in the AR case there should be strong narrowing of the second, third, etc. lines compared with the width in the specular reflection case, which is due to the longer path traveled by the effective electrons responsible for the gently sloping wing of the electron focusing line. Consequently, the profile of the electron focusing line should be more symmetric. Figure 4c shows the results of a calculation carried out using the geometric model of electron focusing allowing for the probability that an electron reaches C for different values of l, demonstrating the validity of the above ideas.

The dashed curve in Fig. 2 gives the results of the calculation of electron focusing for the multiple AR case, in satisfactory agreement with the experimental results. It is worth noting the experimentally observed enhancement of the monotonic behavior in the region of the electron focusing lines with high numbers compared with the calculations. One of the possible reasons for such behavior is the cutoff of the AR at low angles of incidence.[21,22] Grazing electrons, which are reflected specularly, determine the unbalance between electrons and holes at C in high fields H.

ENERGY DEPENDENCE OF THE ANDREEV REFLECTION PROBABILITY

Generation of nonequilibrium excitations. Under conditions such that $l(\varepsilon) \gg b$ (Shavrin probe) when a microjunction is formed by a single crystal filling the space containing a thin nonconducting membrane with a small aperture b_E, under a voltage $U_E^=$ the distribution function of electrons in the region of the aperture has the form shown in Fig. 5 (Ref. 23). If $kT \ll |eU_E^=|$, $|eU_E^=|$, modulation of the voltage at the junction results in periodic generation of nonequilibrium electrons with an excitation energy such that

$$|e(|U_E^=| - U_E^=)| \lesssim \varepsilon \lesssim |e(|U_E^=| + U_E^=)|.$$

If $l(\varepsilon) \gtrsim L$ and $U_E^= \ll |U_E^=|$, a modulation technique makes it possible to observe electron focusing due to excitations of energy $\approx |eU_E^=|$. When ε is increased, we have a situation when $l(\varepsilon) \gg b$, but $l(\varepsilon) < L$. If an electron focusing line is due to focusing of excitations of energy ε, then its amplitude observed on increase in $|U_E^=|$ should fall proportionally to $\propto \exp[-\lambda_0/l(\varepsilon)]$, where λ_0 is the path traveled by an ef-
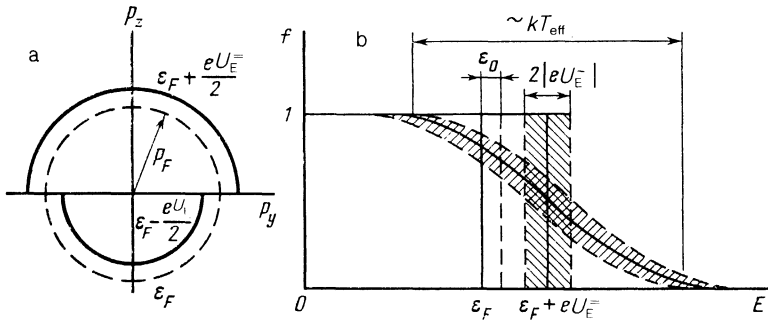
FIG. 5. Electron distribution function in the region of an aperture (emitter) near the plane of a membrane: a) the continuous curve separates the occupied from the vacant states at $T = 0$ (the p_z axis is directed along the normal to the membrane plane); b) fixed directions when $T = 0$ and $T \neq 0$. The shaded regions represent the states of nonequilibrium electrons generated periodically by modulation of the emitter voltage.

fective electron from E to C as a result of focusing. At low values of $|U_E^=|$ a shift of an electron focusing line on the scale of H, due to the difference between the momentum of the focused electrons from p_F, should be linear and the amplitude should be independent of the polarity of $U_E^=$.

Characteristic dependences of the amplitude of the first focusing line and of its position on the H scale on the value of the current $I_E^=$ are shown in Fig. 6a. In the range $I_E = <0.5$ mA the line shift is a linear function of $I_E^=$. The position of the electron focusing line in this region can be used to determine the scale along the ε axis ($\varepsilon_F = 21$ meV—Ref. 24). The amplitude of the electron focusing line depends on the polarity of the $I_E^=$. The dependence of the shift of the line and of its amplitude on the polarity of $I_E^=$ is in particular due to the magnetic field of the emitter current. In the case shown in Fig. 6 when the current is 1 mA, its magnetic field near E reaches several oersted and the field for the observation of the first electron focusing line is 23 Oe. Naturally, in the determination of $l(\varepsilon)$ we can use the average value of the amplitude of the electron focusing line obtained for different polarities of $I_E^=$. In the range $\varepsilon \lesssim 1$ meV the dependence of the amplitude on ε is described well by the expression

$$A(\varepsilon) \propto \exp(-\lambda_0 \alpha \varepsilon^2)$$

[represented by the dashed curve in Fig. 6a where $l(\varepsilon) = 500 \ [\mu m \cdot meV^2]/\varepsilon^2$ [meV]; at 1 meV the value obtained is ~ 10 times greater than that determined from the cyclotron resonance.[25] On further increase in $U_E^=$ there is no radical reduction in the amplitude of the electron focusing line, but it changes continuously (up to $U_E^= = 100$ mV). Such a dependence and the very fact of observation of electron focusing at such high acceleration voltages are due to

phase-matched generation of excitations of energy $\lesssim \varepsilon_0$ [$l(\varepsilon_0) \approx \lambda_0$] in the vicinity of E during relaxation of strongly nonequilibrium excitations. This results, in particular, in local heating of the emitter region which undoubtedly occurs at sufficiently high voltages $U_E^=$. For the sake of simplicity we shall assume that all the voltages $U_E^=$ are of the acceleration type, i.e., that $\varepsilon' = |U_E^=|$ (see Fig. 5). We shall introduce a temperature T_{eff} which represents heating and depends on $U_E^=$, rising when the voltage is increased. The situation is very different in the two cases when

$$kT_{eff} \ll \varepsilon', \quad |\varepsilon' - \varepsilon_0|$$

and when this condition is disobeyed. If

$$kT_{eff} \ll \varepsilon', \quad |\varepsilon' - \varepsilon_0|,$$

then electrons responsible for the focusing line have the energy

$$\varepsilon \approx \varepsilon', \quad A \propto \exp[-\lambda_0/l(\varepsilon)].$$

When the above condition is disobeyed, because excitations have energies in the range $\sim kT_{eff}$ (see Fig. 5), then generation of excitations of energy less than ε_0 is possible even for $\varepsilon' > \varepsilon_0$. Consequently, a deviation should be observed from the exponential dependence of A. The curves in Fig. 6b illustrate the situation. The calculations allow for the thermal broadening of the distribution function and for the normalization factor [$-\lambda_0/l(\varepsilon)$]. Qualitatively the change in the dependence of A on $U_E^=$ due to local heating corresponds to that observed experimentally, but a quantitative comparison shows that there is an additional mechanism of phase-matched generation of nonequilibrium excitations characterized by an energy $\varepsilon \lesssim \varepsilon_0$, i.e., in a region of size $\sim b$ in the
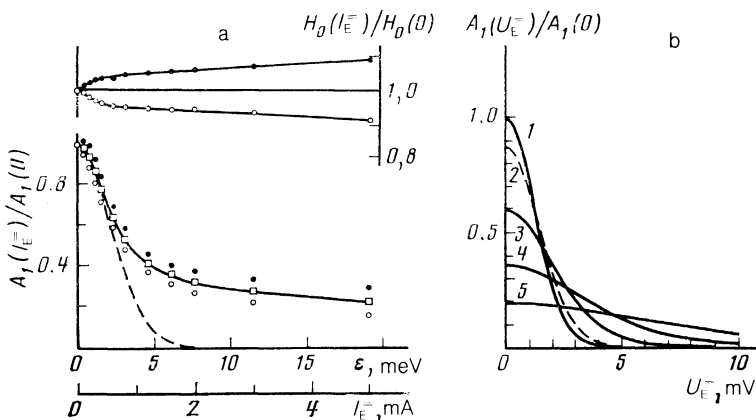
FIG. 6. a) Dependences of the positions (two upper curves) and amplitudes of the first electron focusing line (in relative units) on $I_E^=$; $L = 43 \ \mu m$. The symbols ● and ○ denote the data obtained for different polarities of $I_E^=$; □ represents the average value of the amplitude. The dashed curve is calculated using $A_1(\varepsilon)/A_1(0) = \exp(-0.12\varepsilon^2)$, where ε is in milielectron-volts. b) Dependence of the amplitude of the electron focusing line on $U_E^=$ obtained at different effective temperatures T_{eff} (K); 1) 0; 2) 4.6; 3) 11.6; 4) 23.2; 5) 46.4.

vicinity of E the process of relaxation of excitations of energy $\varepsilon > \varepsilon_0$ leads to generation in this region of excitations of energy $\lesssim \varepsilon_0$.

The fall of the amplitude of an electron-focusing line on increase in $U_E^=$ during recording of $U_C^=$ in the range of small values of L ($< 100 \mu m$) is observed practically always, but the degree of the fall depends strongly on poorly controlled features such as the position of a point electrode and the state of the surface. For example, it was found that when the contact was established for the second time (by raising the point and dropping it again), such a fall decreased strongly. A strong fall could not be observed when a tin film was present on the surface. The fall was found only when a point electrode was placed first on a "perfect" part of the surface of the sample. This indicated that the structural quality of the contact region of a point electrode played an important role in this process. It was established experimentally that defects appeared only in the direct vicinity of a point electrode and the size of the defective region was much less than L.

In this scheme the polarity of $U_E^=$ was unimportant. However, there are several other factors why the polarity of $U_E^=$ can be important. We shall now list some of them. 1) The case when the current density in microjunctions is such that the drift velocity of electrons usually exceeds the velocity of sound. For a contact diameter of $1 \mu m$ the drift velocity is comparable with the velocity of sound when the current is $\sim 10^{-4}$ A. Consequently, when electrons emit phonons continuously, the latter are either focused in the region of E or are defocused in the bulk of the sample, which should alter significantly the temperature conditions in a microjunction depending on the polarity of $U_E^=$. 2) As shown in Ref. 26, in the case of bismuth near a microjunction the mean free path of electrons is very short ($\sim 10^{-5}$ cm), i.e., the diffusion of electrons occurs in the contact region. The effective path traveled by electrons in this region is $\sim b_{eff}^2 / l_i$, where b_{eff} is the characteristic size of the effective region and l_i is the distance traveled by an electron between elastic collisions. The procedure of establishing contacts determines both l_i (defect concentration) and b_{eff}, which thus covers the distance traveled by an electron in the defective region. If $b_{eff}^2 / l_i > L$, the maximum energy of an effective electron is such that $l(\varepsilon) = b_{eff}^2 / l_i$. This is clearly the reason for variation of the energy of the injected electrons under a given acceleration voltage after second contact, for different contacts, etc. The ponderomotive force should shift this "cloud" through which the electric current is flowing; the shift should be either in the direction of C or in the opposite direction, depending on the polarity of $U_E^=$, i.e., L should increase or decrease depending on the polarity of E and this involves a shift of an electron focusing line on the scale of H. 3) The emitter current field has either a focusing or a defocusing effect on a beam of electrons, depending on the polarity of $U_E^=$.

It therefore follows that the results in Fig. 6a demonstrate that if $L \approx 50 \mu m$, we indeed observe focusing of excitations characterized by $\varepsilon \lesssim 1$ meV. In the range of these energies the amplitude of an electron focusing line falls exponentially and the shift of the line on the scale of the field H is linear for both polarities of $U_E^=$.

Role of the sample temperature. In the above discussion of the AR the electron distribution function was considered

at zero temperature. A characteristic scale of the change in the energy in our problem is Δ, which is the energy gap in the spectrum of excitations in the interior of the superconductor, and in a detailed analysis of the dependence of the AR probability on ε we have to ensure that $kT \ll \Delta$. At finite temperatures we find that again q_A differs from Q_A. Naturally, in the first approximation we can assume that at $T \neq 0$ the nonequilibrium distribution function exhibits the same thermal spread as the equilibrium function, and the emitter E generates excitations with energies in the interval $eU_E^= \pm kT$, which determines the difference between q_A and Q_A. Subject to the assumptions made above, we can allow for the circumstances as follows. Under an acceleration voltage $U_E^=$ the electron distribution function is

$$f(E, eU_E^=) = f_0(E - eU_E^=),$$

where f_0 is the Fermi distribution function at a temperature T. Then the fraction of particles that undergo the AR is

$$N(U_E^=) = \int_{-\infty}^{+\infty}\left(-\frac{\partial f}{\partial E}\right) Q_A(\varepsilon)\,dE \bigg/ \int_{-\infty}^{+\infty}\left(-\frac{\partial f}{\partial E}\right) dE.$$

Since we are interested in the fraction of electrons undergoing the AR and making a contribution to the amplitude of an electron focusing line, the integration limits should be replaced as follows:

$$N(U_E^=) = \int_{\varepsilon_F + eU_E - \delta}^{\varepsilon_F + eU_E + \delta}\left(-\frac{\partial f}{\partial E}\right) Q_A(\varepsilon)\,dE \bigg/$$

$$\int_{\varepsilon_F + eU_E - \delta}^{\varepsilon_F + eU_E + \delta}\left(-\frac{\partial f}{\partial E}\right) dE,$$

where the quantity δ is governed by the values of b and L, and by the electron dispersion. If $kT \ll \varepsilon_F$, $\varepsilon \sim kT$, this change in the integration limits has practically no effect. Curves 1–3 in Fig. 7 illustrate the deviation of $q_A(\varepsilon')$ from $Q_A(\varepsilon)$ at various temperatures. It is clear from this figure that only for $T = 1.3$ K (and, consequently, at lower temperatures T) we have $q_A = Q_A$ when $U_E^= = 0$, whereas a 10% deviation of q_A from Q_A occurs for $eU_E^= = 0.6\Delta$.
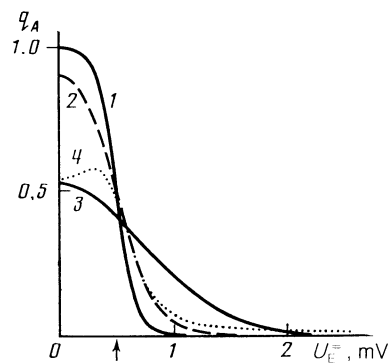
FIG. 7. Calculated dependences $q_A(U_E^=)$. Curves 1–3 are calculated for $Q_A(\varepsilon) = 1, \varepsilon < \Delta$, $Q_A(\varepsilon) = 0, \varepsilon > \Delta$; and $\Delta = 5.9$ K. The temperature T is assumed to be 1.3 K (curve 1), 2.0 K (curve 2), and 5.9 K (curve 3). The dashed curve (4) represents values of $q_A(U_E^=)$ calculated [for $\Delta = 5.9$ K, $T = 1.3$ K, and $Q_A(\varepsilon)$] from Eq. (2) assuming that $B = 2^{1/2}$. The arrow identifies the value of Δ.
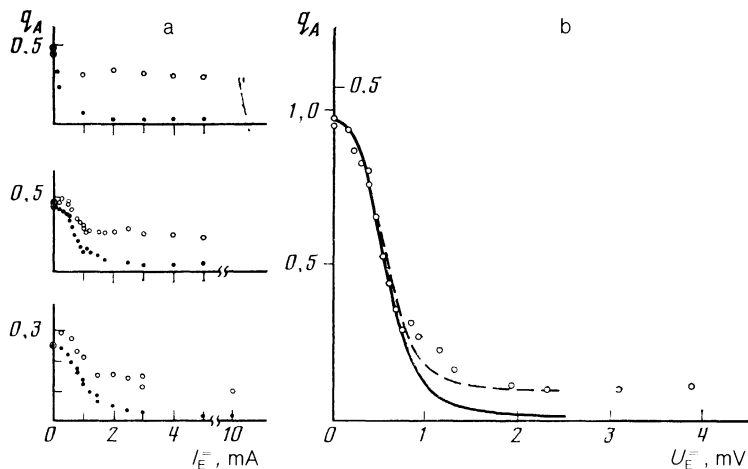
FIG. 8. Dependence of q_A on $U_E^=$ for different polarities of $U_E^=$. Different symbols represent measurements carried out on different parts of the surface of a sample: a) $q_A(I_E^=)$ when $I_E^= < 0$, ($\bullet$), $q_A(I_E^=)$ when $I_E^= > 0$, (O); b) $q_A(U_E^=)$ for $U_E^= < 0$ (O). The continuous and dashed curves give the values of $q_A(U_E^=)$ calculated for $\Delta = 5.9$ K, $T = 1.7$ K, and $Q_A(\varepsilon)$ deduced from Eq. (2) on the assumption that $B = 1$. In the case of the dashed curve the ordinate scale and the beginning of the coordinates are selected so that for $U_E^= = 0$ it coincides with the continuous curve, whereas for $eU_E^= \gg \Delta$ it coincides with the experimental points. The scale for the experimental points is shown on the right of the ordinate, whereas that for the calculated dependence $q_A(U_E^=)$ (continuous curve) is shown on the left.

A strong influence of the relationship between kT and Δ on $q_A(\varepsilon')$ provides an additional method for investigating $Q_A(\varepsilon)$ with the aid of electron focusing. When the dependence of Δ on T is known, a change in T results in a corresponding change in the relationship between kT and Δ. It is possible to determine $Q_A(\varepsilon)$, since this function governs the dependence of $q_A(\varepsilon')$ on the relationship between kT and Δ.

Energy dependence of Q_A on reflection from the Bi–Sn interface. One of the advantages of the electron focusing method for the determination of the AR probability is that the ratio of the amplitudes of two lines, which determines q_A, is independent of l since the path traveled by the effective electrons from E to C is practically the same for these lines and the paths are similar (naturally, under the assumption that the relaxation times of electron and hole excitations are the same).

The range of energies in which it is convenient to investigate $Q_A(\varepsilon)$ by the electron focusing method is governed by the condition $l(\varepsilon) \gtrsim L$. The experimental results demonstrate clearly the dependence of q_A on $U_E^=$ only in the range $L \lesssim 100\,\mu$m, and this dependence is affected strongly by the polarity. Figure 8a shows the dependences $q_A(U_E^=)$ obtained in the range $L < 100\,\mu$m for different polarities of $U_E^=$ when electrons are generated and an increase in $|eU_E^=|$ results in a stronger fall of the amplitude of the second electron focusing line than the fall in the case of generation of holes.

If $L = 0.2$–0.6 mm, an increase in $|eU_E^=|$ results in characteristic changes in the profile of the first electron focusing line which is shifted toward higher or lower fields, depending on the polarity of $U_E^=$ (Ref. 18). The increase in $|eU_E^=|$ is accompanied by some reduction in q_A (usually in the interval 0–10 meV); a further rise of $|eU_E^=|$ right up to ε_F or higher has no influence on q_A. This means that the energy of focused excitations does not change significantly in spite of a change in the electron focusing line profile and a shift of the line on the H scale. Some reduction in q_A is clearly due to the heating of the emitter part of the sample (see above). The change in $U_C^=$ (H) due to the absence of an n–s interface reverses the polarity of the even lines.

In the simplest case the difference between the superconducting and normal phases is simply that in the normal phase ($z < 0$) the energy gap vanishes, whereas in the superconducting phase ($z > 0$) it changes abruptly to Δ and remains constant [$\partial\Delta(z)/\partial z = 0$ at $z \neq 0$]. The dependence

$Q_A(\varepsilon)$ was determined for this case by Andreev[27] and it is of the form

$$Q_A(\varepsilon) = 1, \qquad\qquad \varepsilon \leqslant \Delta,$$
$$Q_A(\varepsilon) = \{\varepsilon/\Delta - [(\varepsilon/\Delta)^2 - 1]^{1/2}\}^2, \quad \varepsilon > \Delta. \qquad (1)$$

A calculation of $Q_A(\varepsilon)$ for a specific case of a change in $\Delta(z)$ at $z > 0$ is reported in Ref. 28.

A potential barrier may appear when different substances are in contact at an n–s interface. The energy dependence of the AR, in the presence of a δ-like potential barrier characterized by $\mathcal{H}\delta(z)$ and $\partial\Delta(z)/\partial z = 0$ at $z \neq 0$, is given in Refs. 29 and 30:

$$Q_A(\varepsilon) = \{(\varepsilon/\Delta)^2 + [1 - (\varepsilon/\Delta)^2]B^2\}^{-1}, \quad \varepsilon \leqslant \Delta,$$
$$Q_A(\varepsilon) = \{\varepsilon/\Delta + [(\varepsilon/\Delta)^2 - 1]^{1/2}B\}^{-2}, \quad \varepsilon > \Delta, \qquad (2)$$

where $B = 1 + 2y^2$, $y = \mathcal{H}/\hbar v_F$ and v_F is the Fermi velocity. A general analysis of the problem in the case of a thin potential barrier [$\Delta(z) = 0$ for $z < 0$ and $\partial\Delta(z)/\partial z = 0$ for $z > 0$] in the "pure" limit is given in Refs. 31 and 32. The problem is solved numerically in Ref. 13 allowing for the proximity effect.

In the case of an arbitrary dependence $\Delta(z)$ the characteristic features of the function $Q_A(\varepsilon)$ are as follows. In the absence of the barrier we have $Q_A(0) = 1$, whereas the presence of the barrier produces $Q_A(0)$. The increase in $\Delta(z = 0)$ in the normal metal is opposite to the influence of the potential barrier. When ε increases, so does $Q_A(\varepsilon)$ and it reaches 1 when $\varepsilon \approx \Delta$. On further increase of ε in the range $\varepsilon > \Delta$, we find that $Q_A(\varepsilon)$ decreases to zero at a rate which increases on increase in the difference $\Delta - \Delta(z = 0)$ in a superconductor. Therefore, generally speaking, Eq. (2) describes satisfactorily the dependence $Q_A(\varepsilon)$ for an arbitrary behavior of the order parameter near the interface.

There are a number of factors which hinder a detailed determination of $Q_A(\varepsilon)$ with the aid of electron focusing.[1] The value of $|eU_E^=|$ usually differs from the excitation energy ε, which is due to the method used in the fabrication of microjunctions. When a microjunction is made by filling with a "perfect" single crystal of the space separated by a flat thin impermeable membrane with an aperture characterized by a diameter b_E, we find that $\varepsilon = eU_E^=$ (Ref. 23). We can calibrate $eU_E^=$ using the circumstance that as soon as ε ex-
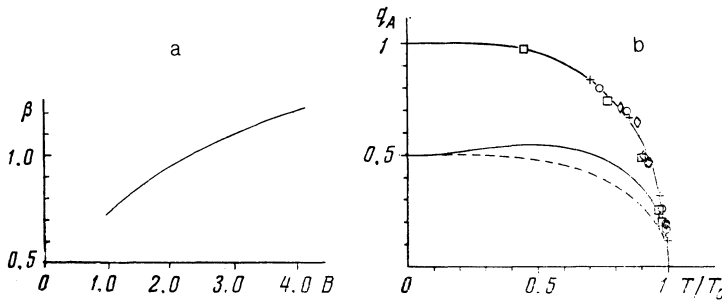
FIG. 9. a) Dependence $\beta(B) = q_A(T_1, B)/q_A(T_2, B)$ calculated for $T_1 = 2.7$ K, $T_2 = 1.3$ K, $\Delta = 5.9$ K, and $Q_A(\varepsilon)$ using Eq. (2). b) Dependence $q_A(T/T_c)$ calculated for $B = 1$ (upper continuous curve) or $B = 2^{1/2}$ (lower continuous curve). The dashed curve represents the upper continuous curve compressed twofold along the ordinate; the symbols represent different series of measurements and the ordinate scale for each series is selected to ensure that the experimental points fit the dependence calculated for $B = 1$.

ceeds Δ, the value of $Q_A(\varepsilon)$ falls steeply. We recall that we have to satisfy the relationship $l(\varepsilon) \gtrsim L$ and if this cannot be done, then additional errors are introduced in the determination of ε from $eU_E^=$.[2] At helium temperatures the condition $kT \ll \Delta$ cannot usually be satisfied (in our case we found that $\Delta/kT \lesssim 4.5$). This means that the energy resolution is low ($\sim T$) and that it is governed by the nonmonoenergetic nature of the electron beam.

The quantity Q_A, which is statistical for the investigated surface, can be found from q_A allowing for the possibility of the island nature of the n–s interface and to establish whether the reduction in $q_A(0)$ compared with 1 is a consequence of the island nature of the film or whether it is due to the presence of a potential barrier at the n–s interface. The following circumstance can be used for this purpose. Firstly, since $Q_A(\varepsilon) = 1$ when $\varepsilon \approx \Delta$ irrespective of the dependence $\Delta(z)$, the quantity $q_A(\varepsilon)$ should exhibit a peak near $\varepsilon = \Delta$ for $Q_A(0) < 1$. Curve 4 in Fig. 7 gives the calculated dependence of $q_A(\varepsilon')$ for $Q_A(\varepsilon)$ in the form of Eq. (2) with $B = 2^{1/2}$. Secondly, measurements of $q_A(0)$ at different temperatures provide additional information on $Q_A(0)$: the values of B and T determine the ratio

$$\beta = q_A(0, T_1)/q_A(0, T_2),$$

so that when β, T_1, and T_2 are known we can find B, i.e., we can deduce the coefficient

$$\gamma = q_A(0)/Q_A(0).$$

Figure 9a shows the calculated dependence of β on B; T_1 and T_2 are, respectively, 2.7 and 1.3 K. Thirdly, $Q_A(\varepsilon)$ governs the temperature dependence $q_A(\varepsilon')$. Figure 9b shows the dependences $q_A(T/T_c)$ calculated for $B = 1$ and $B = 2^{1/2}$ when $|eU_E^=| \ll kT$. The dependence $q_A(T/T_c)$ found for $B = 1$ is practically identical with the dependence $\Delta(T/T_c)/\Delta(0)$ (Ref. 3), which is due to the fact that an electron focusing line resulting from the AR is entirely due to excitations of energy $\varepsilon \ll \Delta$ lying within an energy interval $\sim kT$. Figure 9b shows the experimental dependences $q_A(T/T_c)$ gained under various conditions, including those in Ref. 3. A suitable choice of the scale along the ordinate for each series of measurements makes it possible to describe all the experimental results satisfactorily by the dependence $q_A(T/T_c)$ with $B = 1$. By way of illustration of the influence of the value of B on the dependence $q_A(T/T_c)$ we plotted the curve for $B = 1$ (shown dashed) on such a scale that $q_A(0)$ and $q_A(1)$ are identical with the corresponding quantities when $B = 2^{1/2}$.

The values of $Q_A(\varepsilon)$ were determined for the Bi–Sn in-

terface in one series of measurements in which the dependence $q_A(\varepsilon')$ was manifested most strongly when the emitter generated electron excitations. The analytic expression for $Q_A(\varepsilon)$ was assumed to be given by Eq. (2). The value of $Q_A(0)$ was assumed to be 1. Figure 8b shows, for the sake of comparison, the calculated dependence $q_A(\varepsilon')$ (curves) for the selected form of $Q_A(\varepsilon)$ as well as the experimental results (points). The considerable discrepancy between the calculations and experiments in the range $\varepsilon > \Delta$ is due to phase-matched generation of excitations of energy $< \Delta$ in the region of the emitter E, particularly due to the heating of the region around the emitter. When this is allowed for, we find that the agreement between the experiment and calculations is good.

CONCLUSIONS

We shall now consider some possible investigations by the method described above.

1. It should be possible to determine the Andreev reflection probability for $\varepsilon \ll \Delta$, which should reveal and help to find the height of a potential barrier at a contact or junction between two materials. Measurements can be carried out on materials when one or both of them are superconductors (and in the latter case when the superconductors have different critical temperatures).

2. The energy dependence of the Andreev reflection probability can be studied for $\varepsilon < \Delta$, which should make it possible to investigate surface electron states near the n–s interface: such states appear when there is a potential barrier at the interface and they give rise to anomalies (oscillations) in the energy dependence of the Andreev reflection probability. The positions of the energy levels are governed by the shape of the potential well, which represents the coordinate dependence of the order parameter and can be used to reconstruct the shape of the potential barrier.

3. A quantum effect in the form of the above-barrier Andreev reflection and its energy dependence can also be studied. The nature of the dependence is governed by the behavior of the order parameter near the interface and this makes it possible to study the coordinate dependence of the order parameter.

4. It is possible to investigate the energy spread of the nonequilibrium electron distribution function and the structure of this function. If the spread is much greater than Δ (for a thermal spread $kT \gg \Delta$), variation of the reference voltage and measurements of the Andreev reflection probability can be used to reconstruct the density of the electron states in the region of broadening of the distribution function.

5. Since modification of the experimental geometry used in observations of electron focusing can ensure reflection of different local groups of electrons on the Fermi surface, the method described above provides an opportunity for the study of the characteristics of the Andreev reflection due to the position of an excitation on the Fermi surface (angle of incidence). It is obviously possible to use the electron focusing technique to determine the cutoff of the Andreev reflection in the case of oblique incidence of excitations on the interface.[21,22] This cutoff should reveal a singularity of the dependence of the collector voltage on H in the form of an asymmetric peak in a field $H \approx (\varepsilon/\varepsilon_F)^{1/2}H_0$.

6. The energy gap in a superconductor can also be determined.

7. The electron distribution function of a superconductor can be found in the ground state.

8. The energy dependence of the relaxation time of excitations can be investigated. The problem is in a sense the inverse of that considered above: the known Andreev reflection probability is used to find the excitation energy.

We shall stress once again the main advantages of the method: firstly, feasibility of an investigation of the reflection of a local group of electrons on the Fermi surface; secondly, ability to generate electron and hole excitations and to vary their energy in a wide range.

The main thrust in developing the methodology, which should make it possible to extend the range of materials, energies, etc, i.e., the range of applications of a method, should be as follows: use should be made of ultralow temperatures and of the lithographic technique. This technique can be used most conveniently and rationally in the form of electron lithography. If electron lithography is used to shape the emitter and collector contacts, it should be possible to form microjunctions with submicron distances between the contacts, which should extend greatly the range of applications of the electron focusing method as a whole (with an opportunity for investigating semiconductors) and particularly in studies of the Andreev reflection.

We take this opportunity to express our gratitude to S. I. Bozhko, A. A. Moskalev, and I. F. Sveklo for their technical help, and to I. N. Zhilyaev for supplying a bismuth single crystal.

[1]V. S. Tsoĭ, Pis'ma Zh. Eksp. Teor. Fiz. 19, 114 (1974) [JETP Lett. 19, 70 (1974)].

[2]V. S. Tsoĭ, in: Conduction Electrons (ed. by M. I. Kaganov and V. S. Edel'man) [in Russian], Nauka, Moscow (1985), p. 329.

[3]S. I. Bozhko, V. S. Tsoĭ, and S. E. Yakovlev, Pis'ma Zh. Eksp. Teor. Fiz. 36, 123 (1982) [JETP Lett. 36, 153 (1982)].

[4]P. A. M. Benistant, H. van Kempen, and P. Wyder, Phys. Rev. Lett. 51, 817 (1983).

[5]V. S. Tsoĭ and S. E. Yakovlev, Pis'ma Zh. Eksp. Teor. Fiz. 46, 370 (1987) [JETP Lett. 46, 467 (1987)].

[6]I. P. Krylov and Yu. V. Sharvin, Pis'ma Zh. Eksp Teor. Fiz. 12, 102 (1970) [JETP Lett. 12, 71 (1970)].

[7]I. P. Krylov and Yu. V. Sharvin, Zh. Eksp. Teor. Fiz. 64, 946 (1973) [Sov. Phys. JETP 37, 481 (1973)].

[8]S. V. Gudenko and I. P. Krylov, Pis'ma Zh. Eksp. Teor. Fiz. 28, 243 (1978) [JETP Lett. 28, 224 (1978)].

[9]S. V. Gudenko and I. P. Krylov, Zh. Eksp. Teor. Fiz. 86, 2304 (1984) [Sov. Phys. JETP 59, 1343 (1984)].

[10]G. E. Blonder and M. Tinkham, Phys. Rev. B 27, 112 (1983).

[11]P. A. M. Benistant, Doctoral Thesis, University of Nijmegen, Netherlands (1984).

[12]H. F. C. Hoevers, Doctoral Thesis, University of Nijmegen, Netherlands (1987).

[13]P. van Son, Doctoral Thesis, University of Nijmegen, Netherlands (1987).

[14]A. G. Shepelev, O. P. Ledenev, and G. D. Filimonov, Pis'ma Zh. Eksp. Teor. Fiz. 14, 428 (1971) [JETP Lett. 14, 290 (1971)].

[15]V. F. Gantmakher and Yu. V. Sharvin, Prib. Tekh. Eksp. No. 6, 165 (1963).

[16]A. A. Moskalev and V. S. Tsoĭ, Poverkhnost' No. 5, 52 (1985).

[17]V. S. Tsoĭ and N. P. Tsoĭ, Zh. Eksp. Teor. Fiz. 73, 289 (1977) [Sov. Phys. JETP 46, 150 (1977)].

[18]V. S. Tsoĭ, Doctoral Thesis [in Russian], Institute of Solid-State Physics, Academy of Sciences of the USSR, Chernogolovka (1978).

[19]Yu. A. Kolesnichenko, Fiz. Nizk. Temp. 8, 312 (1982) [Sov. J. Low. Temp. Phys. 8, 156 (1982)].

[20]V. S. Tsoĭ, Zh. Eksp. Teor. Fiz. 68, 1849 (1975) [Sov. Phys. JETP 41, 927 (1975)].

[21]Yu. K. Dzhikaev, Zh. Eksp. Teor. Fiz. 68, 295 (1975) [Sov. Phys. JETP 41, 144 (1975)].

[22]L. Yu. Gorelik and A. M. Kadigrobov, Fiz. Nizk. Temp. 7, 131 (1981) [Sov. J. Low. Temp. Phys. 7, 65 (1981)].

[23]A. N. Omel'yanchuk, I. O. Kulik, and R. I. Shekhter, Pis'ma Zh. Eksp. Teor. Fiz. 25, 465 (1977) [JETP Lett. 25, 437 (1977)].

[24]V. S. Édel'man, Usp. Fiz. Nauk 123, 257 (1977) [Sov. Phys. Usp. 20, 819 (1977)].

[25]S. M. Cheremisin, V. S. Édel'man, and M. S. Khaĭkin, Zh. Eksp. Teor. Fiz. 61, 1112 (1971) [Sov. Phys. JETP 34, 594 (1972)].

[26]E. I. Ass and N. N. Gribov, Fiz. Nizk. Temp. 13, 645 (1987) [Sov. J. Low Temp. Phys. 13, 365 (1987)].

[27]A. F. Andreev, Zh. Eksp. Teor. Fiz. 46, 1823 (1964) [Sov. Phys. JETP 19, 1228 (1964)].

[28]J Bar-Sagi, Solid State Commun. 27, 363 (1978).

[29]A. Griffin and J. Demers, Phys. Rev. B 4, 2202 (1971).

[30]G. E. Blonder, M. Tinkham, and T. M. Klapwijk, Phys. Rev. B 25, 4515 (1982).

[31]A. L. Shelankov, Pis'ma Zh. Eksp. Teor. Fiz. 32, 122 (1980) [JETP Lett. 32, 111 (1980)].

[32]A. L. Shelankov, Fiz. Tverd. Tela (Leningrad) 26, 1615 (1984) [Sov. Phys. Solid State 26, 981 (1984)].

Translated by A. Tybulewicz

539   Sov. Phys. JETP 68 (3), March 1989

Tsoĭ et al.   539